Artificial intelligence–based avoidance of hopf bifurcations in dynamic optimal control of fermentation systems

American Journal of Chemistry
Vol. 11, No. 1, 13-34, 2026
e-ISSN:2616-5244

Lakshmi. N. Sridhar

Chemical Engineering Department, University of Puerto Rico, Mayaguez, Puerto Rico, USA.
Email: lakshmin.sridhar@upr.edu

ABSTRACT

In biochemical systems, nonlinear processes are often associated with the Hopf bifurcation, which can result in oscillations, instability, and reduced product concentration. While bifurcation analysis tools such as MATCONT, implemented in MATLAB, can efficiently determine Hopf bifurcation points and associated stability boundaries, the direct incorporation of these results into dynamic optimal control problems remains an area of research. This paper presents an artificial intelligence-based approach for the optimal control of nonlinear biochemical processes. The proposed approach first determines the Hopf bifurcation points using the bifurcation analysis tool MATCONT. A neural network is then developed to determine the dominant eigenvalue or its proximity as an artificial intelligence-based surrogate model. This surrogate model is then incorporated into the optimal control framework based on the Pyomo model. The results demonstrate the efficiency of the proposed approach in maximizing product concentration while ensuring process stability. The proposed approach achieves near-optimal product concentrations, with only a small reduction compared to the unconstrained case, while effectively avoiding Hopf bifurcation-induced oscillations. In addition, the resulting control profiles remain smooth and practically implementable, highlighting the robustness of the proposed framework.

Keywords: *Artificial intelligence, Bifurcation, Control, Fermentation, Hopf, Optimization.*

DOI: 10.55284/ajc.v11i1.1841

Citation | Sridhar, L. N. (2026). Artificial intelligence–based avoidance of hopf bifurcations in dynamic optimal control of fermentation systems. *American Journal of Chemistry, 11*(1), 13–34.

Copyright: © 2026 by the author. This article is an open access article distributed under the terms and conditions of the Creative Commons Attribution (CC BY) license (https://creativecommons.org/licenses/by/4.0/).

Funding: This study received no specific financial support.

Institutional Review Board Statement: This study was approved by the Institutional Review Board of Chemical Engineering Department, University of Puerto Rico, Mayaguez, Puerto Rico, under protocol number [IRB NO. 402053], dated 18 December 2025. Informed verbal consent was obtained from all participants, and all data were anonymized to protect participant confidentiality.

Transparency: The author confirms that the manuscript is an honest, accurate, and transparent account of the study; that no vital features of the study have been omitted; and that any discrepancies from the study as planned have been explained. This study followed all ethical practices during writing.

Competing Interests: The author declares that there are no conflicts of interests regarding the publication of this paper.

History: Received: 19 March 2026/ Revised: 22 May 2026/ Accepted: 29 May 2026/ Published: 5 June 2026

Publisher: Online Science Publishing

Highlights of this paper

- This paper addresses the integration of bifurcation analysis and optimal control in continuous fermentation processes.
- Continuous fermentation processes exhibit oscillatory behavior, which reduces product quality.
- In this work, a strategy is developed to control the processes while avoiding regions where oscillatory behavior can occur.

1. INTRODUCTION

Nonlinear biochemical systems often exhibit complex dynamics, including multiple steady states and self-sustained oscillations arising from Hopf bifurcations. Oscillatory behavior, generally detected by bifurcation analysis using the MATCONT software implemented in MATLAB, may significantly affect the process's efficiency and productivity. During fermentation and other chemical reactions, operating near a Hopf bifurcation point destabilizes the process, leading to periodic fluctuations in key variables and reducing its controllability. Optimum production is not achievable during this period.

The existence of oscillations, periodic cycles, multiplicity regions, and even chaotic behavior in fermentation processes has been widely reported in the literature. Such complex dynamic phenomena arise due to strong nonlinear interactions between microbial growth, substrate consumption, and product formation, and have important implications for process stability and control.

For fermentations involving *Zymomonas mobilis*, these behaviors have been documented in several studies. Early investigations by Jöbses, Egberts, Luyben, and Roels (1986) and Ghommidh, Vaija, Bolarinwa, and Navarro (1989) identified oscillatory dynamics and multiple steady states. Subsequent work by Bruce, Axford, Ciszek, and Daugulis (1991) and Daugulis, McLellan, and Li (1997) further explored the nonlinear behavior and its dependence on operating conditions, while more recent studies by Garhyan and Elnashaie (2004) and Mahecha-Botero, Garhyan, and Elnashaie (2006) examined bifurcation structures and the onset of instability.

Similarly, oscillatory behavior has been extensively studied in fermentations involving *Saccharomyces cerevisiae*. Foundational work by Von Meyenburg (1973) highlighted the role of metabolic regulation, while later studies such as Perego Jr et al. (1985) and Mulchandani and Volesky (1986) investigated dynamic responses under varying environmental conditions. Additional contributions by Parulekar, Semones, Rolf, Lievense, and Lim (1986), Strässle, Sonnleitner, and Fiechter (1989), Martegani, Porro, Ranzi, and Alberghina (1990) and Beuse, Bartling, Kopmann, Diekmann, and Thoma (1998) further characterized oscillations and their underlying mechanisms.

The Jones and Kompala (1999) widely used to describe the fermentation of *S. cerevisiae*, has been shown computationally to exhibit oscillatory dynamics, as demonstrated by Simpson, Kompala, and Meiss (2009). Over the past decade, significant efforts have focused on optimizing and controlling bioreactors exhibiting such oscillatory behavior. Zhu, Zamamiri, Henson, and Hjortsø (2000) developed model predictive control strategies to stabilize periodic solutions in continuous yeast bioreactors using cell population balance models. Kurtz, Henson, and Hjortsø (2000) proposed a nonlinear control strategy for mixed-culture bioreactors in which two cell populations compete for a single growth-limiting substrate. Parker and Doyle (2001) designed nonlinear model-based controllers to regulate biomass exit concentration in continuous-flow bioreactors.

Further contributions include Zhang, Zamamiri, Henson, and Hjortsø (2002) who employed an unstructured segregated model to analyze bifurcations leading to periodic solutions and to develop feedback linearizing controllers. Mhaskar, Hjortsø, and Henson (2002) introduced a segregated model with a structured description of the extracellular environment, enabling parameter identification from measurable extracellular variables. Gadkar, III, Crowley, and Varner (2003) presented a cybernetic model of polyhydroxybutyrate synthesis in a continuous

bioreactor integrated with model predictive control. Zhang, Henson, and Kevrekidis (2003) performed nonlinear model reduction for dynamic analysis of *S. cerevisiae* fermentation and demonstrated that reduced-order models can capture the long-term behavior of the full system. Henson (2003) and Henson (2005) further demonstrated the utility of cell population models and metabolically structured ensembles for dynamic analysis and model-based control of glycolytic and respiratory oscillations.

Although numerous studies have established the presence of oscillatory dynamics, relatively few have addressed systematic strategies for their elimination. Suppressing oscillations is of practical importance because they increase residual sugar concentrations, thereby reducing ethanol yield—potentially by as much as fifty percent (Bai, 2007). Oscillatory behavior also negatively affects ethanol productivity and reactor operability (Zhang & Henson, 2001) and dynamic instabilities may pose safety concerns while compromising overall process efficiency.

Sridhar (2011) proposed simple and effective strategies to eliminate oscillatory behavior in continuous fermentation systems. It was shown that, for the *Zymomonas mobilis* process, introducing a small fraction of components from the product stream suppressed Hopf bifurcations and eliminated sustained oscillations. In Saccharomyces cerevisiae, increasing the inlet oxygen concentration produced a similar stabilizing effect. Moreover, an equivalent stabilization could be obtained by increasing the oxygen mass transfer coefficient, thereby enhancing oxygen availability within the reactor.

The limit cycles of continuous fermentation processes with Zymomonas mobilis and Saccharomyces cerevisiae are undesirable because they induce sustained oscillations in critical state variables, including biomass, substrate, product, and dissolved oxygen concentrations. The sustained oscillations prevent the continuous process from operating at a steady optimal condition and force the process to continually deviate from the desired operating point.

In continuous ethanol fermentation processes with Zymomonas mobilis (Garhyan & Elnashaie, 2004) sustained oscillations can create conditions that lead to periodic buildup of residual sugars. During some periods of the cycle, the substrate is used inefficiently, reducing the process's overall efficiency and lowering ethanol yields. The overall productivity of the continuous process is, on average, significantly lower than under steady-state conditions. Additionally, sustained oscillations in biomass concentration can affect the overall predictability of the process.

In Saccharomyces cerevisiae (Simpson et al., 2009) oscillations have often been reported to result from interactions between glycolytic metabolism and oxygen levels. These dynamic instabilities result in oscillations between aerobic and anaerobic metabolism, reducing the process's efficiency and leading to oscillations in ethanol production rates. These instabilities also reduce the ease with which the process can be monitored and controlled, since controllers are typically designed for steady-state operation.

In addition to reductions in yield and productivity, limit cycles have also been reported to cause process difficulties, including increased energy consumption, mechanical stress, and safety risks, particularly with regard to gas evolution. The elimination of oscillatory instabilities is therefore critical for a stable, efficient, and viable process.

2. MATERIALS AND METHODS

The main aim of this work is to perform optimal control calculations using artificial intelligence to avoid limit-cycle-causing Hopf Bifurcations. The rationale for using artificial intelligence to avoid Hopf bifurcations detected by MATCONT in MATLAB stems from the strong relationship between stability and optimal productivity in nonlinear bioprocesses. A Hopf bifurcation represents the initiation of sustained oscillations, resulting in the creation of limit cycles, diminished steady-state products, and difficulties in the implementation of optimal control

policies. Although MATCONT can accurately detect bifurcations offline, integrating stability analysis directly into a dynamic optimal control approach in PYOMO is computationally expensive, given the need to repeatedly perform eigenvalue analyses on large nonlinear models.

Artificial intelligence can play a significant role in addressing this challenge. A trained artificial intelligence model can estimate the dominant eigenvalue or detect proximity to a Hopf bifurcation as a smooth, continuously differentiable function of the bioprocess states and inputs. This stability surrogate can be easily incorporated into the objective function of the Pyomo optimization model as a penalty or constraint, enabling the optimal control strategy to avoid oscillatory regimes and maximize the concentration of the products of interest in a computationally efficient manner.

The present work aims to develop an artificial intelligence-assisted optimal control strategy that helps avoid the Hopf bifurcation domain while maximizing production in biochemical systems. Bifurcation points are first accurately identified using the MATCONT software in MATLAB to determine the stability domains of nonlinear biochemical systems. A neural network is developed to determine the process's stability domain by approximating the stability function. The developed function is used to formulate an optimal control strategy via the Pyomo software package, considering the stability domain while maximizing production in biochemical systems.

This paper is organized as follows. First, the model equations for continuous fermentation processes involving Zymomonas Mobilis and Saccharomyces cerevisiae are presented. This is followed by a description of the bifurcation analysis, optimal control, and the neural network procedures. The results discussion and conclusions are then presented.

The novelty of this work lies in the combination and integration of bifurcation analysis, artificial intelligence, and optimal control, using bifurcation analysis to predict Hopf Bifurcation points, neural networks to develop constraints to avoid Hopf bifurcation, and optimal control to achieve the optimal result.

2.1. Zymomonas Fermentation Process

For the continuous fermentation problem involving Zymomonas Mobilis, the dynamic model (Garhyan & Elnashaie, 2004) for the 4 components, substrate (S), the key compound (e) , microorganism or biomass (X), and product (P) are given by the following equations.

$$\begin{aligned}
\frac{dC_e}{dt} &= \bar{D}(C_{e0} - C_e) + [k_1 - k_2 C_P + k_3 C_P^2](\frac{C_S C_e}{K_S + C_S}) \\
\frac{dC_X}{dt} &= \bar{D}(C_{X0} - C_X) + P(\frac{C_S C_e}{K_S + C_S}) \\
\frac{dC_S}{dt} &= -m_S C_X + \bar{D}(C_{S0} - C_S) - \mathrm{P}(\frac{1}{Y_{SX}})(\frac{C_S C_e}{K_S + C_S}) \\
\frac{dC_P}{dt} &= m_P C_X + \bar{D}(C_{P0} - C_P) + \mathrm{P}(\frac{1}{Y_{PX}})(\frac{C_S C_e}{K_S + C_S})
\end{aligned} \tag{1}$$

D is the dilution rate. Table 1 has all the parameter values.

Table 1. Base set of parameters used for the *Zymomonas Mobilis* fermentation.

Parameter	Value
K_1	16.0
K_2	0.497
K_3	0.00383
Y_{px}	0.0526315
K_s	0.5
P	0.1283
ms	2.16
mp	1.1
Ysx	0.02444498

Source: Sridhar (2011).

2.2. Saccharomyces Cerevisiae Fermentation Process

The *Saccharomyces Cerevisiae* fermentation process was originally modeled by Jones and Kompala (1999) and analyzed by Simpson et al. (2009). For three available pathways r_i, the cybernetic variables $u_i$and v_i represent the optimal strategies for enzyme synthesis and activity. The variables $u_i$and $v_i$are given by the equations

$$u_i = \frac{r_i}{\sum_j r_j} \tag{2}$$

$$v_i = \frac{r_i}{\max_j r_j} \tag{3}$$

while the expressions for the pathways r_i are given by,

$$r_1 = \mu_1 e_1 \frac{G}{K_1 + G} \tag{4}$$

$$r_2 = \mu_2 e_2 \left(\frac{E}{K_2 + E}\right)\left(\frac{O}{K_{O_2} + O}\right) \tag{5}$$

$$r_3 = \mu_3 e_3 \left(\frac{G}{K_3 + G}\right)\left(\frac{O}{K_{O_3} + O}\right) \tag{6}$$

The dynamic equations are given by,

$$\frac{dX}{dt} = X\sum_i r_i v_i - DX$$
$$\frac{dG}{dt} = (G_0 - G)D - (\frac{r_1 v_1}{Y_1} - \frac{r_2 v_2}{Y_2})X - \phi_4(C\frac{dX}{dt} + X\frac{dc}{dt})$$
$$\frac{dE}{dt} = -DE + (\phi_1\frac{r_1 v_1}{Y_1} - \frac{r_2 v_2}{Y_2})X$$
$$\frac{dO}{dt} = k_L a(O^* - O) - (\phi_2\frac{r_2 v_2}{Y_2} + \phi_3\frac{r_3 v_3}{Y_3})X \quad (7)$$
$$\frac{de_i}{dt} = \alpha u_i\frac{S_i}{K_i + S_i} - (\sum_j r_j v_j + \beta)e_i + \alpha^*$$
$$\frac{dC}{dt} = \gamma_3 r_3 v_3 - (\gamma_1 r_1 v_1 + \gamma_2 r_2 v_2)C - \sum_i (r_i v_i)C$$

The concentrations of glucose, ethanol and dissolved oxygen are given by G, E, O. $\mu_i$represents the modified growth rate constant. K_i and represent the saturation constants for the carbon substrate and the dissolved oxygen for each metabolic pathway. The inlet glucose feed concentration is G_0, X is the cell mass concentration and $k_L a$ represents the mass transfer coefficient for dissolved oxygen. $\alpha$and β represent the enzyme synthesis and decay rate constants while Y is the yield coefficient. The stoichiometric coefficients for the intercellular storage carbohydrate synthesis and consumption are given by ϕ_i and γ_i. Table 2 gives the base values of the variables and constants used.

Table 2. Base set of parameters used for the Saccharomyces Cerevisiae fermentation problem.

Parameter	Value
G_0	10 gm/l
Y_1, Y_2, Y_3	(0.16, 0.75, 0.6) gg^{-1}
$\phi_1, \phi_2, \phi_3, \phi_4$	0.403, 2, 1, 0.95
O^*	7.5 mg/l
α	0.3
α^*	0.1
β	0.7
K_1, K_2, K_3	0.05, 0.01, 0.001
K_{O_2}	0.01mg/l
K_{O_3}	2.2 mg/l
$\gamma_i (i = 1,2,3)$	10, 10, 0.8
$\mu_{i,\max} (i = 1,2,3)$	0.44, 0.19, 0.36

3. BIFURCATION ANALYSIS AND OPTIMAL CONTROL

3.1. Bifurcation Analysis

Bifurcation calculations are performed using the MATLAB software MATCONT. Bifurcation analysis explains the main causes for multiple steady-states and limit cycles. Branch points and limit points cause multiple steady-state solutions while limit cycles and oscillatory behavior are causd by Hopf bifurcation points. The MATLAB program that effectively locates limit points, branch points, and Hopf bifurcation points is MATCONT. This

program was developed and improved by several researhers (Dhooge, Govaerts, & Kuznetsov, 2003; Dhooge, Govaerts, Kuznetsov, Mestrom, & Riet, 2003). This program is very effective in identifying Limit points(LP), branch points(BP), and Hopf bifurcation points(H) for an system of ordinary differential equations.

$$\frac{dx}{dt} = f(x, \alpha) \tag{8}$$

$x \in R^n$ where the bifurcation parameter is α . The gradient vesctor is orthogonal to the tangent and hence the tangent plane at any point $w = [w_1, w_2, w_3, w_4, \ldots . w_{n+1}]$ must satisfy.

$$Aw = 0 \tag{9}$$

The matrix A is defined by

$$A = [\partial f / \partial x \quad | \partial f / \partial \alpha] \tag{10}$$

The sub-matrix $\partial f / \partial x$ is the Jacobian matrix. For both limit and branch points, the Jacobian matrix $J = (\partial f / \partial x)$ must have a determinant of 0.

At a limit point, the $n+1^{th}$ component of the tangent vector $w_{n+1} = 0$. For a branch point, the matrix $B = \begin{bmatrix} A \\ w^T \end{bmatrix}$ must be singular and have a determinant of 0.

At a Hopf bifurcation point,

$$\det(2 f_x(x, \alpha) @ I_n) = 0 \tag{11}$$

@ indicates the bialternate product while I_n is the n-square identity matrix. Hopf bifurcations cause limit cycles and should be eliminated because limit cycles make optimization and control tasks very difficult. More details can be found in Kuznetsov (1998); Kuznetsov (2009) and Govaerts (2000) respectively.

3.2. Optimal Control

Pyomo.dae Hart et al. (2017) is used for the Optimal Control calculations. Pyomo.DAE is a powerful extension of the Pyomo optimization modeling framework, which is well-suited for solving dynamic systems of differential and algebraic equations. It is a symbolic environment for solving differential-algebraic equation systems in the context of optimization problems. This is very important in process systems engineering, chemical kinetics, and control systems, where the dynamic response of systems is of prime interest.

At its heart, Pyomo.DAE enables users to define time-varying variables, derivatives, and constraints symbolically, which can be easily integrated into a Pyomo model. Users can easily define continuous sets for time or other continuous variables, which can be used to define their derivatives over those sets. This symbolic approach enables users to easily discretize continuous differential-algebraic equation systems using finite difference, collocation, or orthogonal collocation methods, thereby transforming continuous differential equations into algebraic equations that can be solved with standard solvers. The framework can handle both initial-value problems and dynamic optimization problems. In dynamic optimization, Pyomo.DAE allows the formulation of time-dependent objective functions and constraints, which is particularly useful in optimal control, energy systems, and chemical process scheduling problems.

One of the major advantages of Pyomo.DAE is that it is compatible with the Pyomo ecosystem. This allows users to leverage existing solver interfaces, variable bounds, nonlinear constraints, and objective functions within a combined static and dynamic modeling framework. Furthermore, the symbolic framework makes it easier to perform model verification, automatic differentiation, and sensitivity analysis. Pyomo.DAE provides a flexible, extensible, and open-source environment for modeling, simulation, and optimization of dynamic systems. By integrating symbolic modeling of DAEs with powerful discretization and optimization capabilities, it provides a

unique framework for solving complex time-dependent problems. Its tight integration with Pyomo enables the efficient solution of both simple and complex dynamic optimization problems, making it a cornerstone of modern computational modeling of dynamic systems. In Pyomo.DAE , the differential equations are converted to a Nonlinear Program (NLP) using the orthogonal collocation method. The NLP is solved using IPOPT (Wächter & Biegler, 2006).

4. FORMATION OF STABILITY DATASET FROM MATCONT RESULTS

A stability dataset was developed based on the results from numerical continuation calculations carried out in MATCONT. The stability dataset consists of rows, each representing a continuation point from an equilibrium branch. The columns in each row consist of the state variables, the bifurcation parameter, and a stability measure. The stability measure is a numerical value derived from the Jacobian matrix. The Jacobian matrix is computed numerically at each equilibrium point. The eigenvalues are then computed automatically using MATLAB. The maximum value of the real part of these eigenvalues is then computed as a scalar stability measure.

The stability measure is computed using "eig_real_max = max(real(eigvals));" in MATLAB. The stability measure is a quantitative metric in which negative values indicate locally asymptotically stable equilibria, positive values indicate instability, and a zero crossing indicates a Hopf bifurcation. The stability dataset is then saved as a CSV file. The dataset can then be used in subsequent computational calculations to perform classification or regression to identify stability boundaries or approximate bifurcations.

5. NEURAL NETWORK SURROGATE FOR STABILITY PREDICTION

Direct embedding of eigenvalue calculations into IPOPT-based optimal control is impractical for several reasons: (i) computing eigenvalues at each time step is computationally expensive, (ii) the mapping from states to the maximum eigenvalue is non-smooth near eigenvalue crossings, and (iii) symbolic differentiation of eigenvalues is challenging.

Prior to neural network training, all input variables were standardized to improve numerical conditioning and training stability. Let x_{raw} denote the vector of state variables and bifurcation parameter obtained from the stability dataset. For each input variable j, the training mean $\mu_j$and training standard deviation $\sigma_j$were computed over the training dataset as the arithmetic mean and standard deviation, respectively. The training mean for the input variable j is defined as the arithmetic average over all training samples as $\mu_j = \frac{1}{N}\sum_{k=1}^{N} x_j^{(k)}$ and the training standard deviation for the input variable $j$is defined as: $\sigma_j = \frac{1}{N}(\sum_{k=1}^{N} x_j^{(k)} - \mu_j)^2$

The standardized inputs were defined as;

$$x_j = \frac{x_{\text{raw},j} - \mu_j}{\sigma_j}$$

This transformation ensures that each input variable has zero mean and unit variance over the training set, thereby improving neural network conditioning and gradient-based optimization performance.

The vectors μ, σ $\mu$and σ computed during training were stored and embedded identically within the Pyomo optimal control formulation to ensure consistency between neural network training and deployment.

To overcome these limitations, a feedforward neural network is trained to approximate the maximum eigenvalue as a smooth function of the system state and bifurcation parameter. A typical architecture employs the hyperbolic tangent (tanh) as a smooth activation function. If the input vector is denoted by x, which are the scaled variables, then the network is defined as:

$$z1 = tanh(W1\,x + b1)$$
$$z2 = tanh(W2\,z1 + b2) \quad (12)$$
$$\lambda\_max\_NN = W3\,z2 + b3$$

Because tanh is infinitely differentiable, the network is fully smooth, guaranteeing the availability of first and second derivatives required by IPOPT. Here, W1, W2, and W3 are the weights that scale and combine inputs or hidden-layer features, while b1, b2, and b3 are the biases that allow the neurons to shift their activation independently of the inputs. Without biases, the network output would be constrained to pass through the origin, limiting flexibility.

The hidden-layer outputs z1, z2, represent nonlinear combinations of the inputs and previous-layer features, respectively. Each element of z_1 is a smoothed combination of the original inputs, while each element of z2 encodes more abstract patterns extracted from z1. The final output λ_max_NN provides a smooth approximation of the maximum real eigenvalue, enabling efficient and differentiable stability evaluation within the optimal control problem. Figure 1 shows a chart describing the computational strategy.

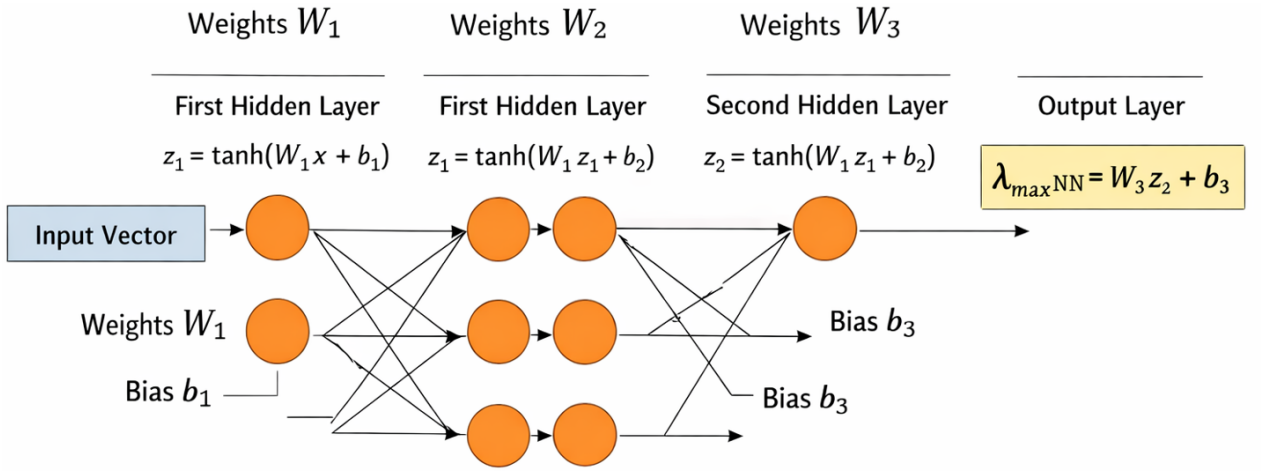

Figure 1. Feed forward neural network diagram.

The schematic illustrates a feedforward neural network used to approximate the maximum real part of the eigenvalues of the system Jacobian as a smooth function of the process variables. The procedure begins with the construction of an input vector, denoted by (x), which contains the relevant state variables of the biochemical system together with the bifurcation or operating parameter, typically the dilution rate. Prior to entering the network, these variables are assumed to be scaled using the training mean and standard deviation so that each input has comparable magnitude, thereby improving numerical conditioning and training performance. The scaled input vector is then passed to the first hidden layer, where it is linearly transformed through multiplication by the weight matrix (W_1) and shifted by the bias vector (b_1). This linear combination represents a weighted aggregation of all input features, allowing each neuron in the first hidden layer to "see" the entire input space. The resulting affine transformation is then passed through the hyperbolic tangent activation function, producing the first set of nonlinear features denoted by (z_1 = \tanh(W_1 x + b_1)). The use of the tanh activation function ensures that the mapping is smooth and infinitely differentiable, which is essential for compatibility with gradient-based optimization algorithms such as IPOPT.

The transformed vector (z_1) serves as the input to the second hidden layer, where a similar operation is performed. Specifically, (z_1) is multiplied by a second weight matrix (W_2) and shifted by a second bias vector

(b_2), forming another affine transformation that combines the nonlinear features extracted in the previous layer. This is again followed by the application of the tanh activation function, yielding the second hidden-layer output (z_2 = \tanh(W_2 z_1 + b_2)). At this stage, the network has constructed higher-level nonlinear representations of the original input variables, capturing complex interactions between the biochemical states and the operating parameter. Each neuron in this layer effectively encodes an abstract feature that contributes to the prediction of system stability.

The final stage of the network is the output layer, which performs a linear combination of the features in (z_2). The vector (z_2) is multiplied by the weight matrix (W_3) and shifted by the bias (b_3), producing a scalar output given by (\lambda_{\text{max,NN}} = W_3 z_2 + b_3). This scalar represents the neural network approximation of the maximum real part of the eigenvalues of the Jacobian matrix. Because no activation function is applied at the output layer, the network is able to produce both positive and negative values, corresponding respectively to unstable and stable operating conditions. A negative value of (\lambda_{\text{max,NN}}) indicates that the system is locally asymptotically stable, whereas a positive value indicates instability. A value near zero corresponds to a critical transition, such as a Hopf bifurcation, where oscillatory dynamics may emerge.

The entire mapping from input vector (x) to output (\lambda_{\text{max,NN}}) is smooth and differentiable due to the use of tanh activation functions and linear transformations. This property is crucial because it allows the neural network to be embedded directly within a dynamic optimization framework. In particular, the predicted eigenvalue can be evaluated at every time point along a trajectory and incorporated into the objective function or constraints without introducing non-smooth behavior. The weights (W_1, W_2, W_3) and biases (b_1, b_2, b_3) are obtained during a prior training phase using data generated from numerical continuation, where the true eigenvalues are computed from the Jacobian matrix. Once trained, the network serves as a surrogate model that rapidly predicts stability information without requiring explicit eigenvalue computations. The arrows in the diagram represent the fully connected nature of the network, indicating that each neuron in one layer is connected to every neuron in the subsequent layer. This dense connectivity allows the network to capture complex nonlinear relationships between inputs and outputs.

Overall, the chart depicts a sequence of transformations in which the original process variables are progressively mapped into higher-dimensional feature spaces and then reduced to a single scalar stability metric. The combination of affine transformations, nonlinear activation functions, and a final linear output layer enables the network to approximate the stability boundary of the system accurately. The resulting model provides a computationally efficient and differentiable approximation of the maximum eigenvalue, making it suitable for integration into optimal control formulations where stability considerations are essential.

The integration into optimal control is done in two ways a) Soft penalty formulation and b) a Hard constraint formulation. formulation For the soft constraint formulation, we use a smooth_max function that converts λ into a smooth, nonnegative penalty that only "activates" when the system is unstable:

$$s_{\max}(\lambda+\varepsilon) = smooth-\max(\lambda+\varepsilon) = \frac{(\lambda+\varepsilon)+\sqrt{(\lambda+\varepsilon)^2+\varepsilon}}{2} \qquad (13)$$

λ is the neural network's predicted maximum eigenvalue at the current state and parameter, while ε is a small positive safety margin to ensure differentiability. The soft penalty formulation involves the new objective function, where the original objective function $(\sum P(t))^2$ is modified to $\sum(P(t) - \alpha.s2_{max}$ $(\sum P(t))$ represents the ethanol (product concentration which is maximized. When no measures are taken, $(\sum P(t))^2$is maximized and when the soft penalty formulation is integrated, o $\sum(P(t) - \alpha.s2_{max}$ in both problems. α controls how aggressively

instability is penalized, and ε prevents numerical issues at exactly $\lambda = 0$ and slightly shifts the stability boundary. $(\sum P(t))^2$ represents the summation of the product concentration (Ethanol).

For the Hard constraint formulation, an additional constraint $\lambda\_max\_NN(t) \leq 0$ is added to the original constraints. This strictly prohibits unstable trajectories. The hard penalty makes the problem infeasible and only the soft penalty is used.

In the optimal control of nonlinear biochemical processes, the hard Hopf constraint is frequently difficult to apply in the sense that the maximal real eigenvalue of the system Jacobian matrix must stay non-positive at all times. However, the process dynamics and constraints may require the system to exhibit transient behavior in the region of mild instability in order to maximize the yield of the desired biochemical product. The hard Hopf constraint may prevent the nonlinear solver from converging in such cases because the trajectory may become infeasible. To extend the hard Hopf formulation and alleviate the aforementioned limitations, we propose the application of a soft Hopf penalty function. The penalty function is directly included in the objective function and is a differentiable function. The application of the soft Hopf penalty function ensures the generation of a trajectory that is physically realistic and feasible. The gradients of the objective function are well behaved for the IPOPT solver, which makes the application of the proposed approach computationally efficient for the optimal control of nonlinear biochemical processes.

6. RESULTS AND DISCUSSION

In the Zymomonas mobilis problem, for a C_{S0} value of 105, a Hopf bifurcation point was identified at (C_e, C_X, C_S, C_P, D) values of (1.860487 1.528864 0.508208 50.417516 0.078700) (Figure 2a). The limit cycle caused by this Hopf Bifurcation point is seen in Figure 2b. For the optimal control, $\sum_{t_{i=0}}^{t_i=t_f}(C_P(t_i))$ was maximized. Initially, no measures were taken to avoid the Hopf bifurcations The obtained value of $\sum_{t_{i=0}}^{t_i=t_f}(C_P(t_i))$ was 221.237.. Subsequently, $\sum_{t_{i=0}}^{t_i=t_f}(C_P(t_i))$ was maximized using the soft Hopf penalty formulation, and the obtained value of $\sum_{t_{i=0}}^{t_i=t_f}(C_P(t_i))$ was 278.664248114147 37. In this case, a more beneficial outcome resulted from avoiding Hopf bifurcation points. The control profile (D) exhibits spikes which was remedied using the Saitzky Golay filter to produce the smoother control profiles(DSG). Figures 2c-2f show the various optimal control profiles.

In the *Saccharomyces Cerevisiae* problem, for a G_0 value of 8.75, a Hopf bifurcation point and 2 limit points were located at $[X, G, E, O, e_1, e_2, e_3, C]$ values of (6.169216 0.002931 0.002715 0.565763 0.118462 0.123656 1.034024 0.733038 0.151711); (6.221180 0.003254 0.003062 0.495063 0.118649 0.125084 1.122298 0.719468 0.151968) and (8.734690 0.010731 0.009741 0.093818 0.140241 0.226120 2.141386 0.128217 0.112838). Figure 3a). The limit cycle caused by this Hopf Bifurcation point is seen in Figure 3b Figure 2b. For the optimal control, $\sum_{t_{i=0}}^{t_i=t_f}(E(t_i))$ was maximized. Initially, no measures were taken to avoid the Hopf bifurcations. The value of $\sum_{t_{i=0}}^{t_i=t_f}(E(t_i))$ was 64.493. Subsequently, $\sum_{t_{i=0}}^{t_i=t_f}(E(t_i))$ was maximized using the soft Hopf penalty formulation and the value of f $\sum_{t_{i=0}}^{t_i=t_f}(E(t_i))$ increased to 79.5005. Again, a more beneficial outcome resulted from avoiding Hopf bifurcation points. The control profile (D) exhibits spikes which was remedied using the Saitzky Golay filter to produce the smoother control profiles(DSG). Figures 3a-3h show the various optimal control profiles.

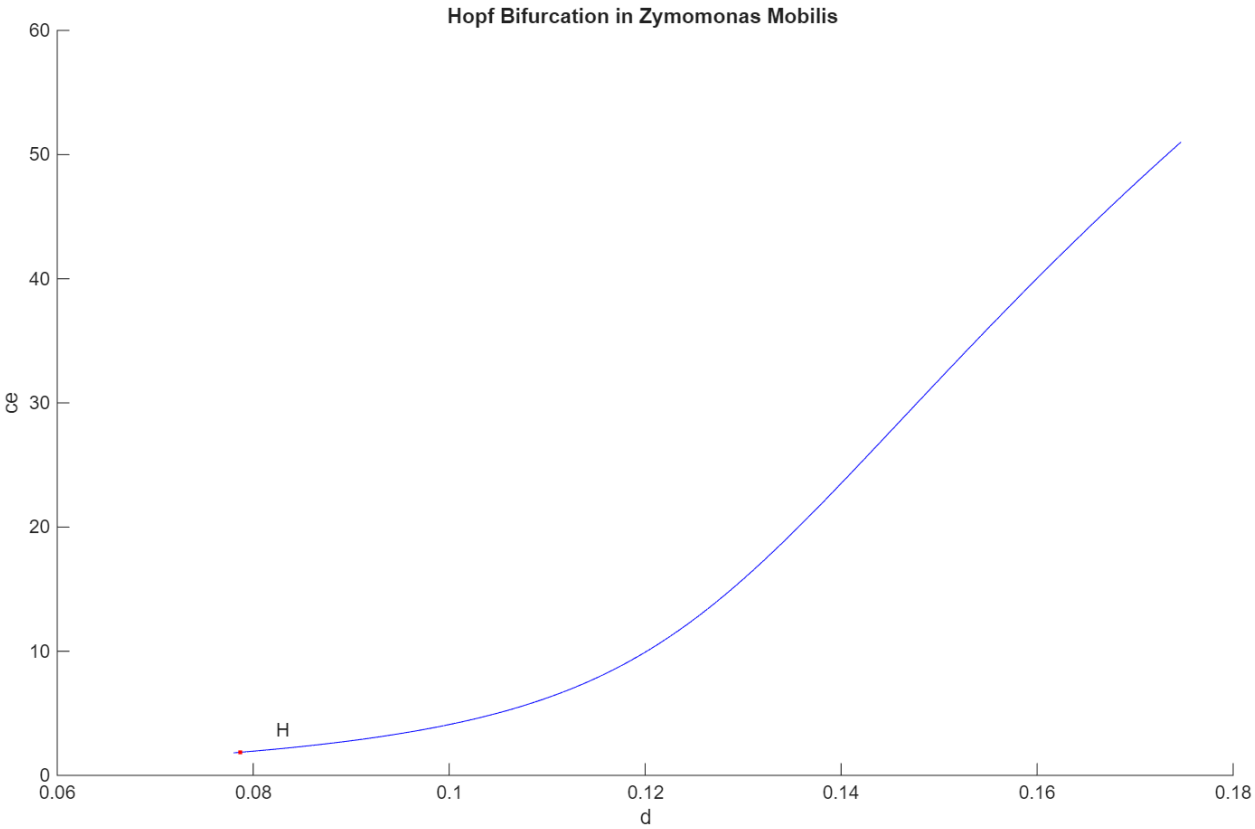

Figure 2a. Hopf bifurcation point for Zymomonas mobilis fermentation problem.

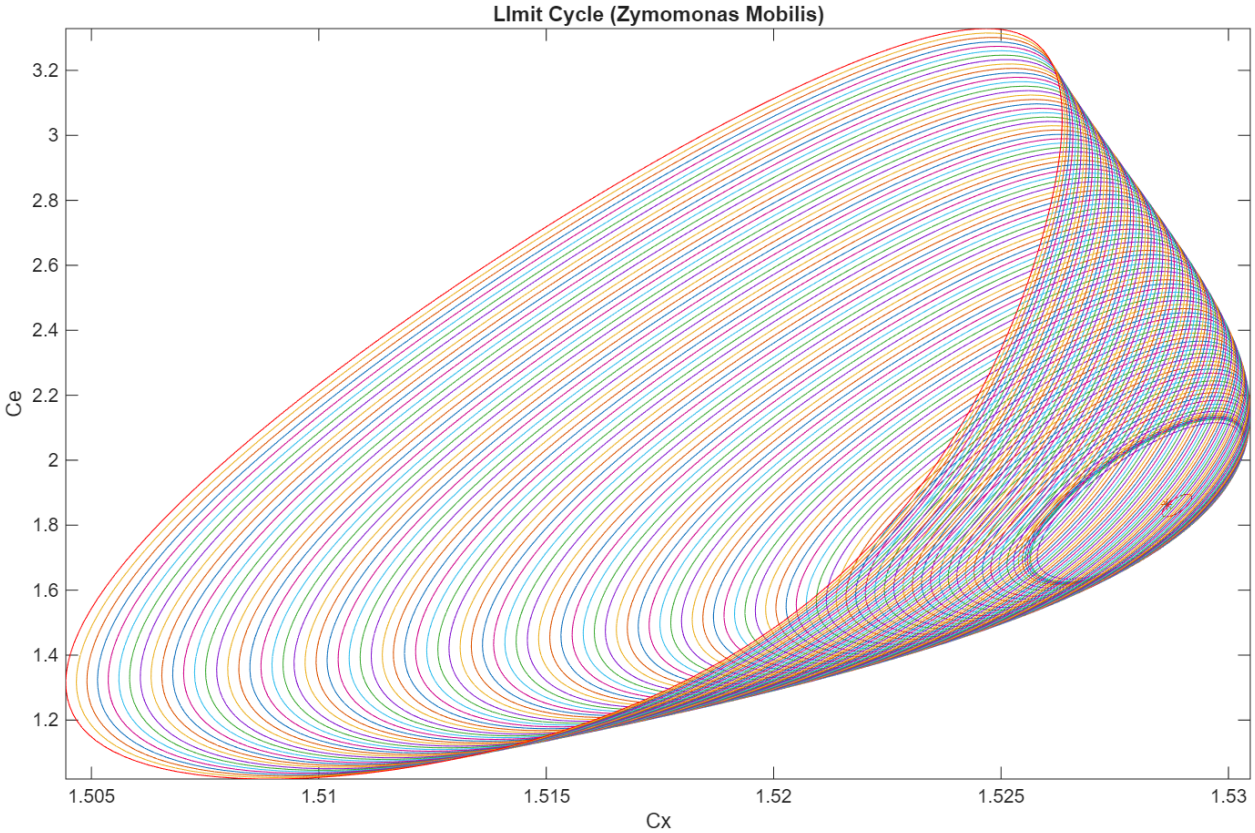

Figure 2b. Limit Cycle for Zymomonas mobilis fermentation problem.

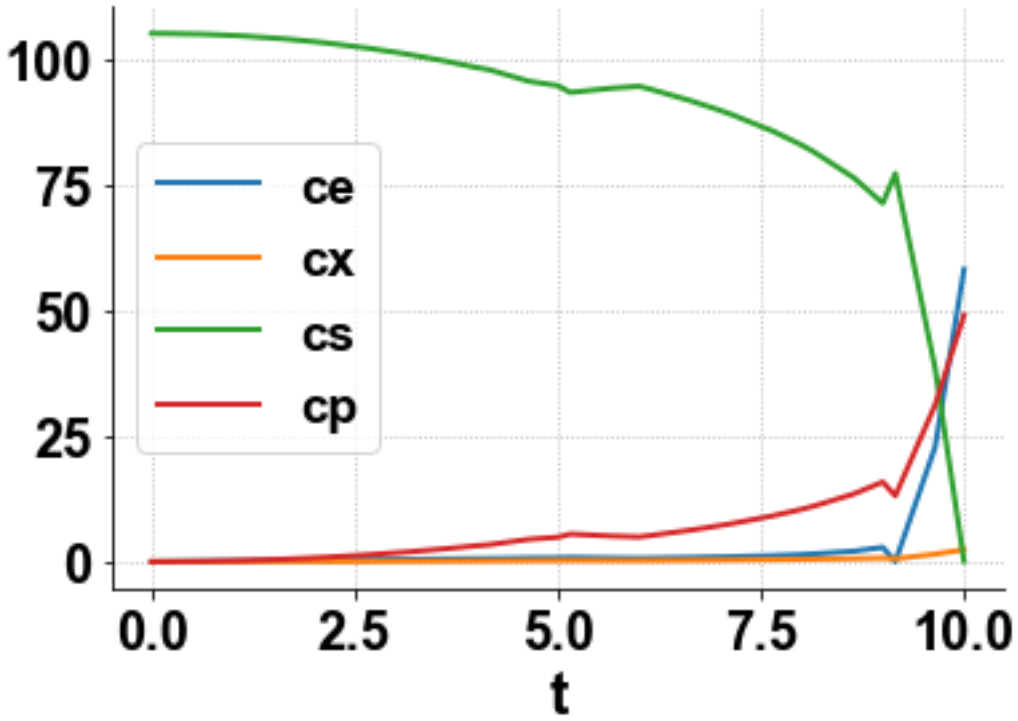

Figure 2c. Optimal control Zymomonas Mobilis concentration profiles (no Hopf panalty).

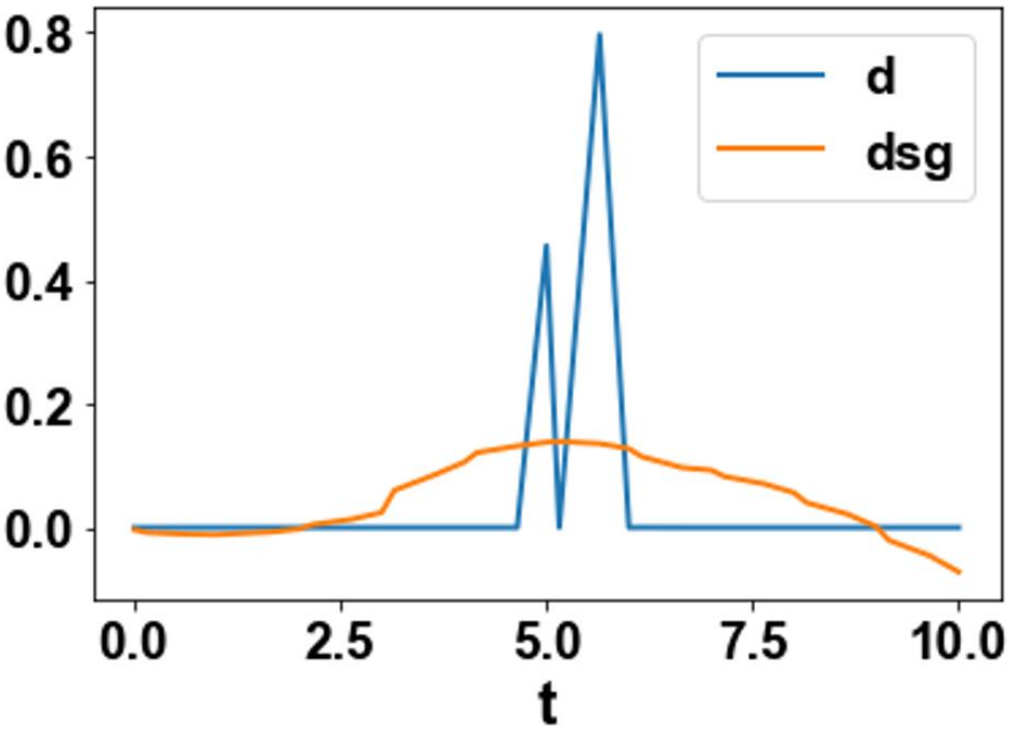

Figure 2d. Optimal control Zymomonas Mobilis (D, Dsg Profiles; no Hopf Penalty).

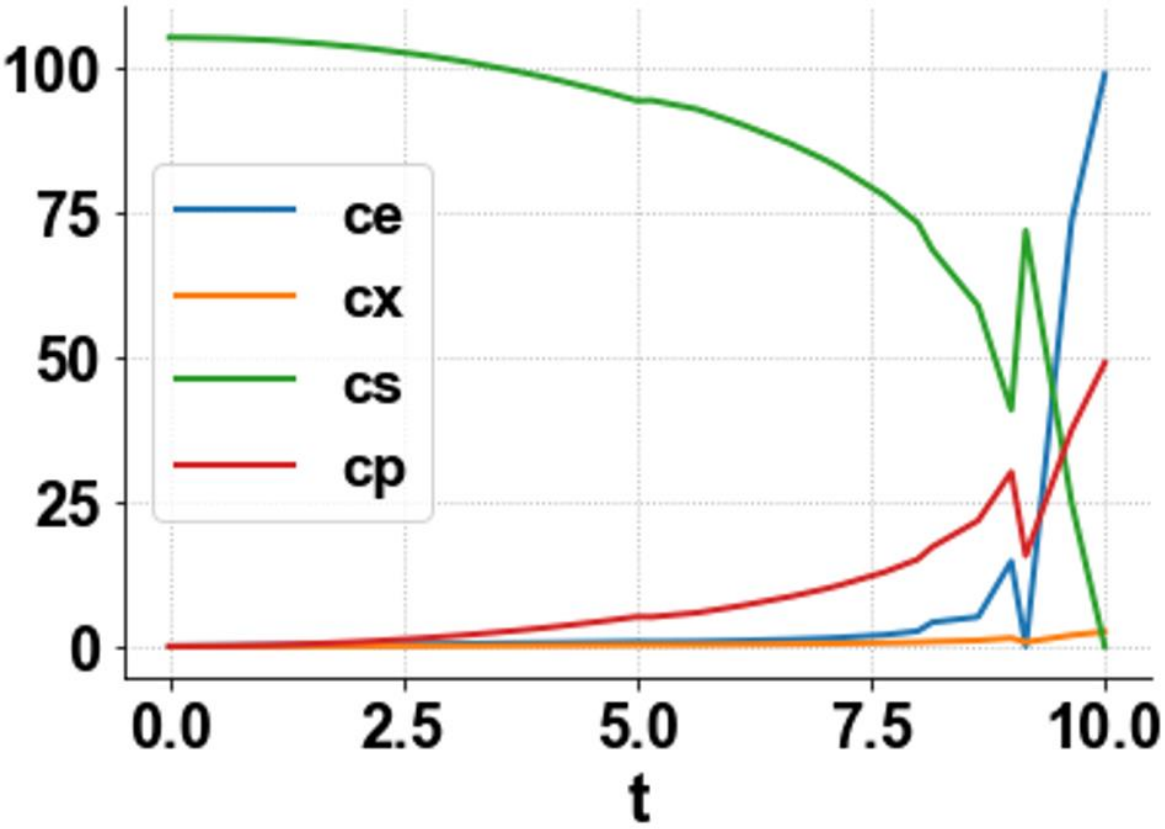

Figure 2e. Optimal control Zymomonas Mobilis concentration profiles (with Hopf panalty).

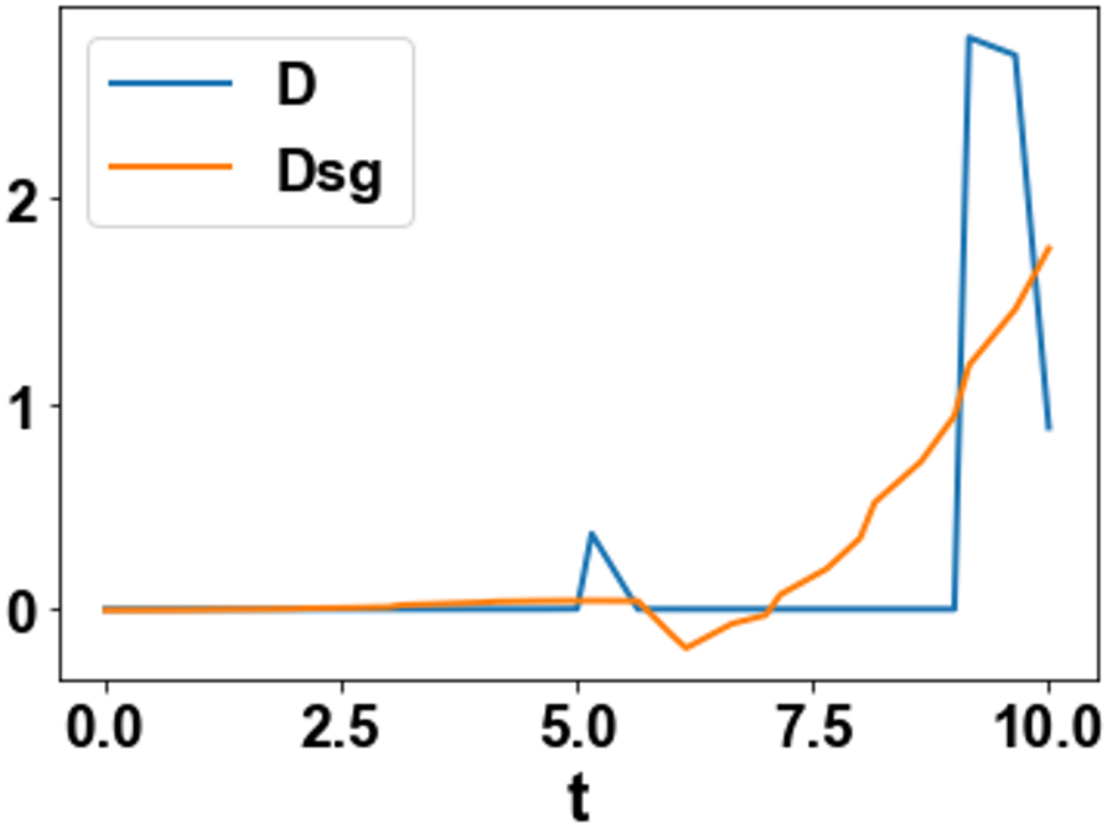

Figure 2f. Optimal control Zymomonas Mobilis (D, Dsg Profiles; with Hopf Penalty).

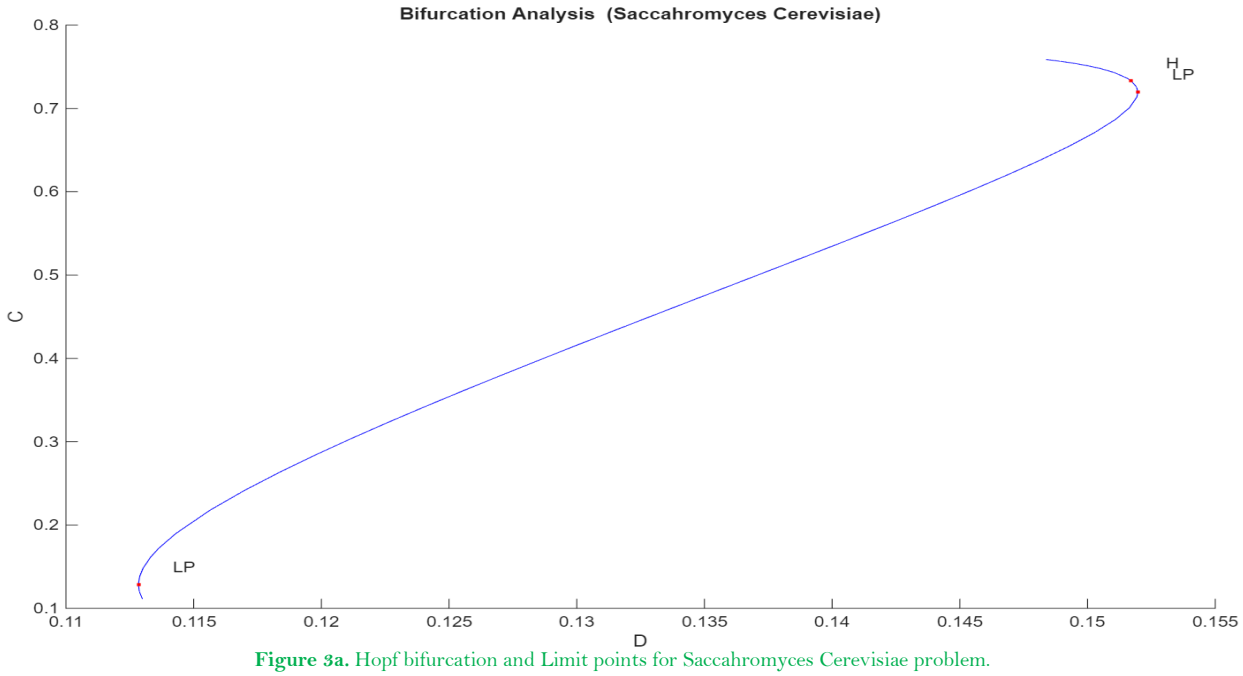

Figure 3a. Hopf bifurcation and Limit points for Saccahromyces Cerevisiae problem.

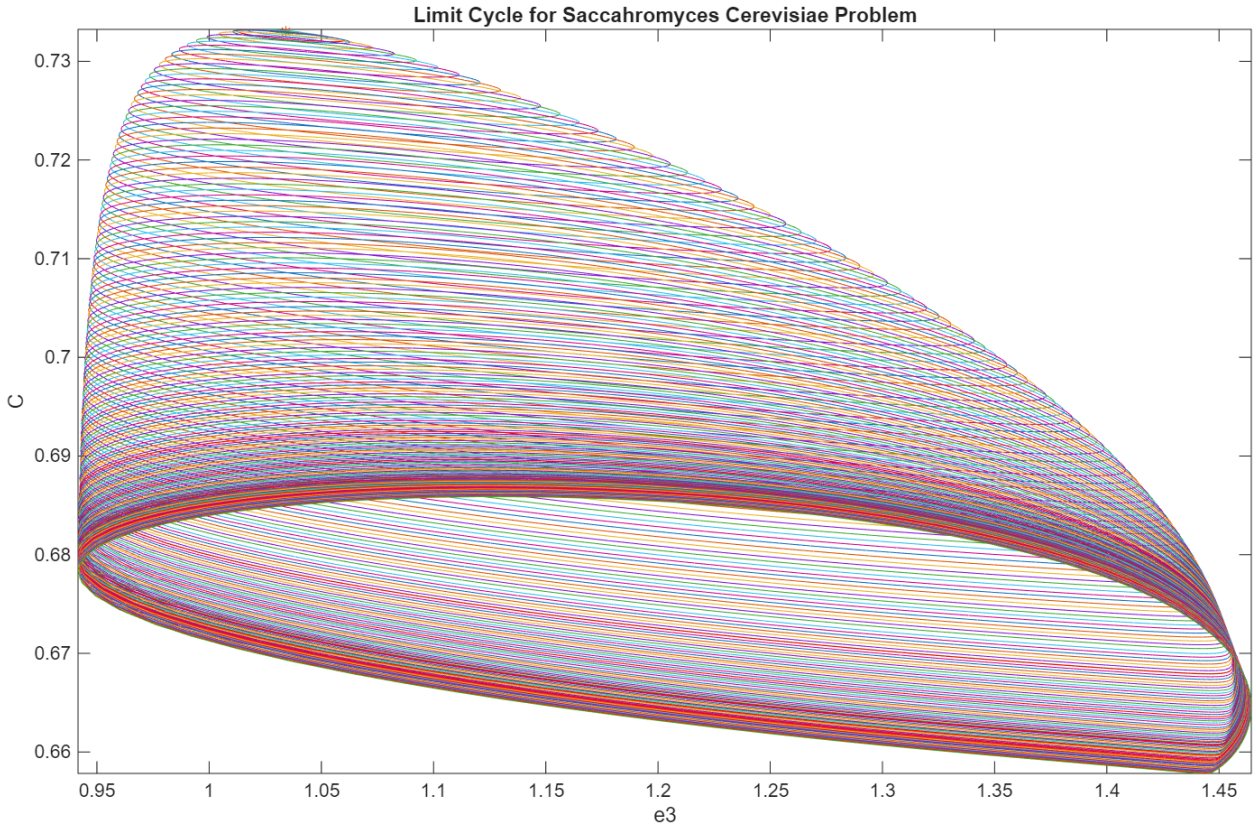

Figure 3b. Limit Cycle for Saccahromyces Cerevisiae problem.

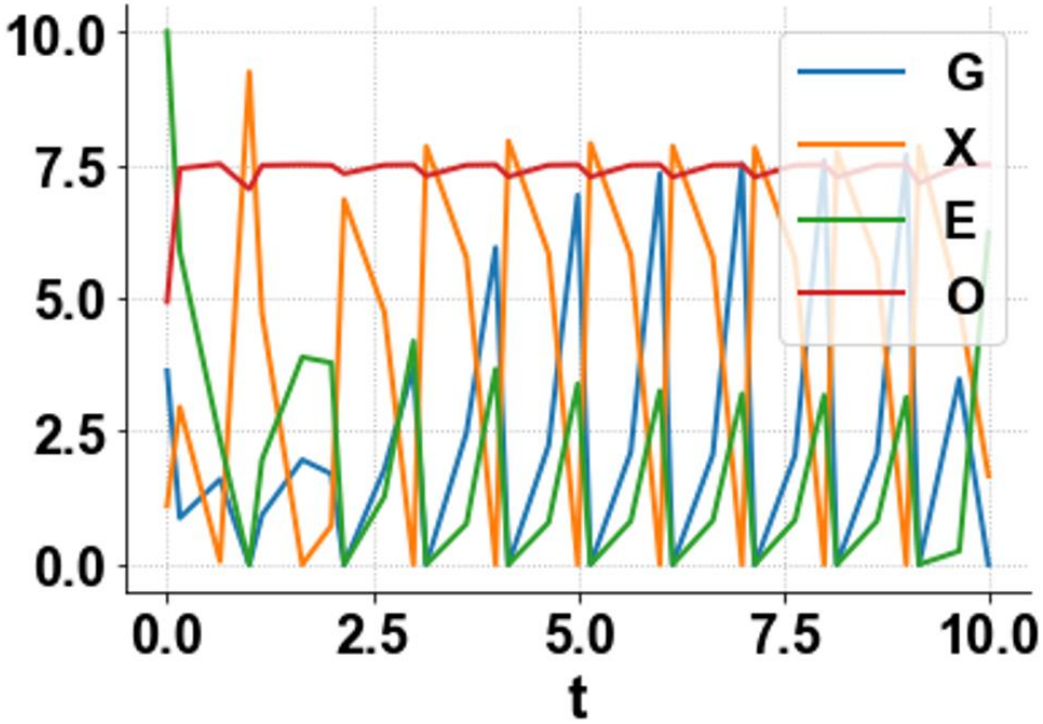

Figure 3c. Optimal Control Saccaharomyces Cerevisiae (G, X, E, O profiles no Hopf penalty).

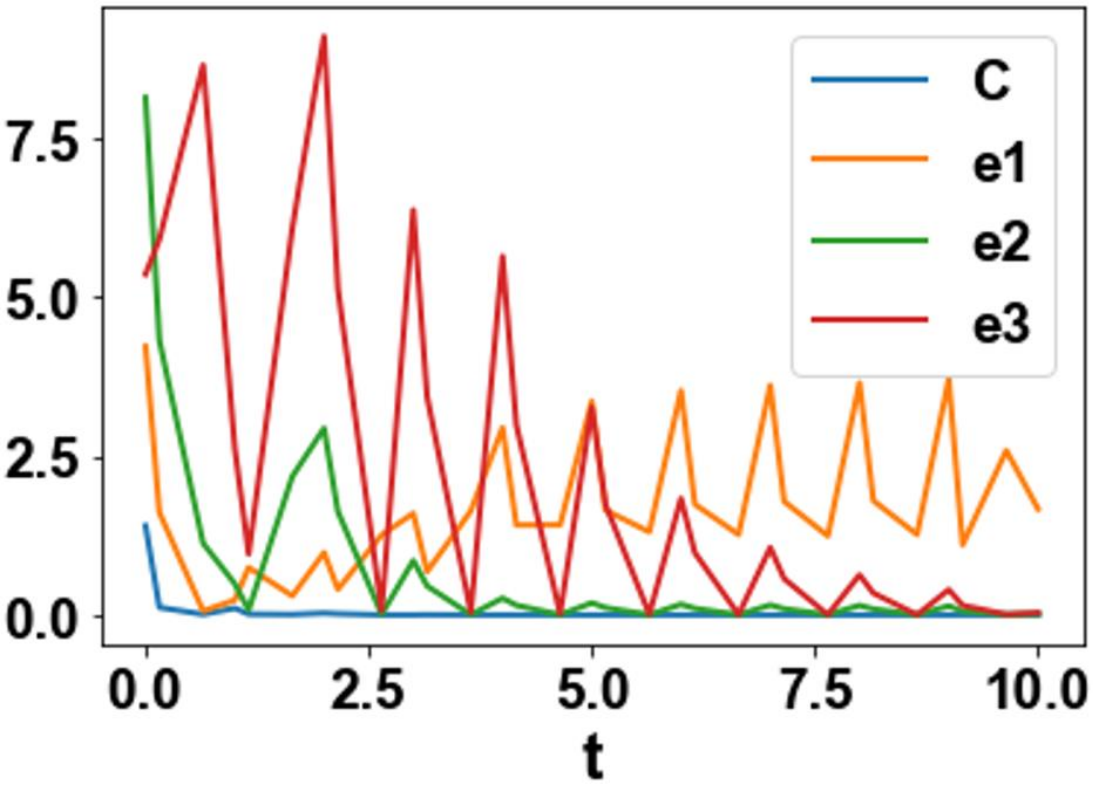

Figure 3d. Optimal Control Saccaharomyces Cerevisiae (C, e1, e2, e3 profiles, no Hopf penalty).

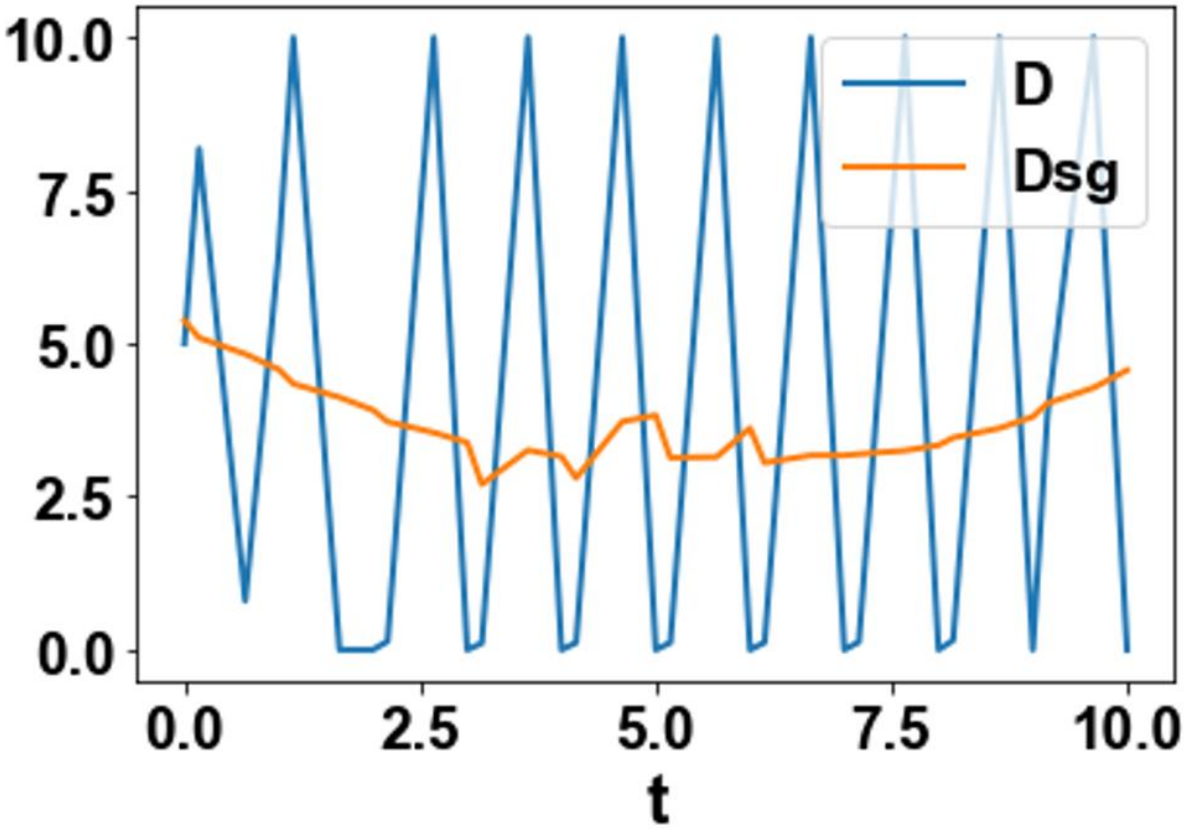

Figure 3e. Optimal Control Saccaharomyces Cerevisiae (D, DSG profiles, no Hopf penalty).

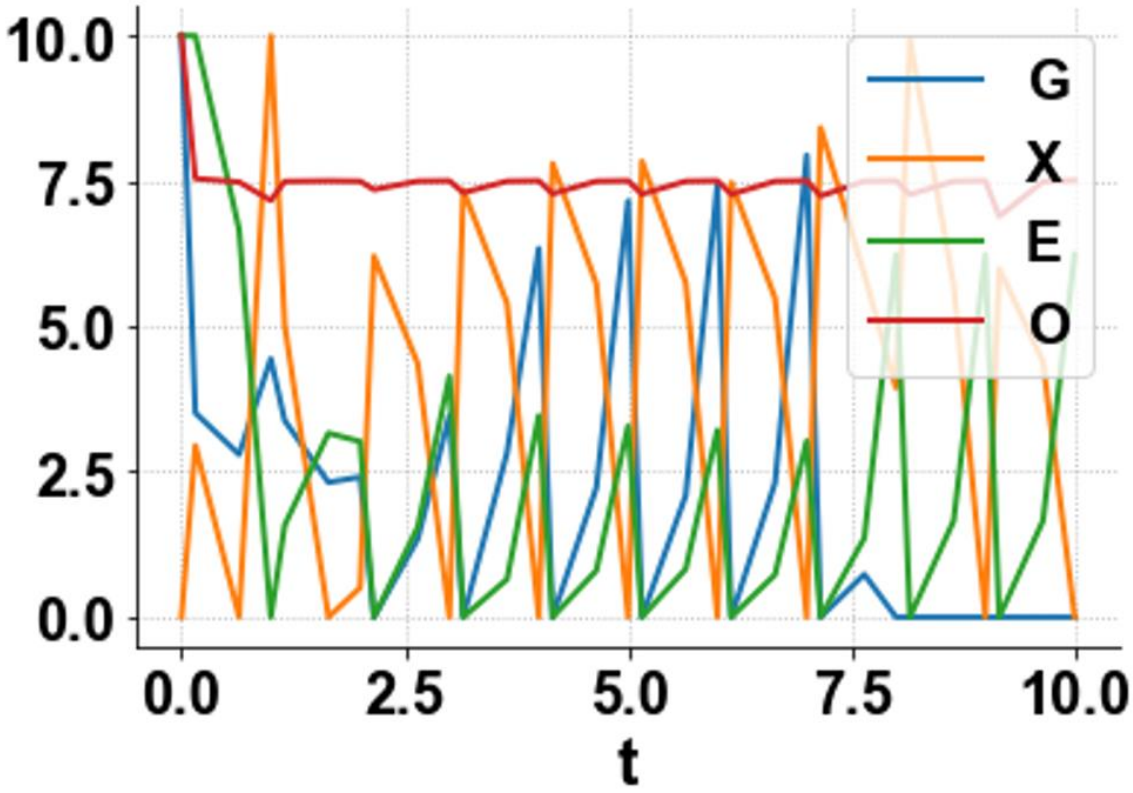

Figure 3f. Optimal Control Saccaharomyces Cerevisiae (G, X, E, O profiles with Hopf penalty).

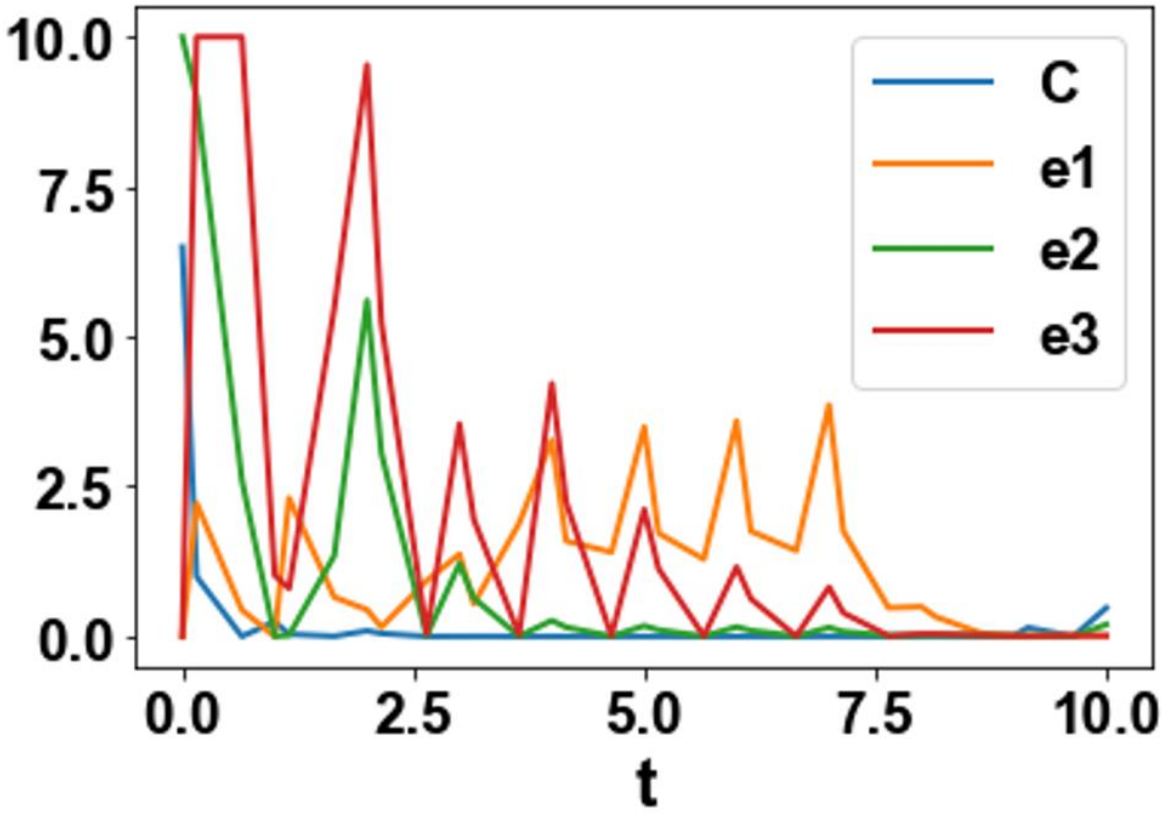

Figure 3g. Optimal Control Saccaharomyces Cerevisiae (C, e1, e2, e3 profiles, with Hopf penalty).

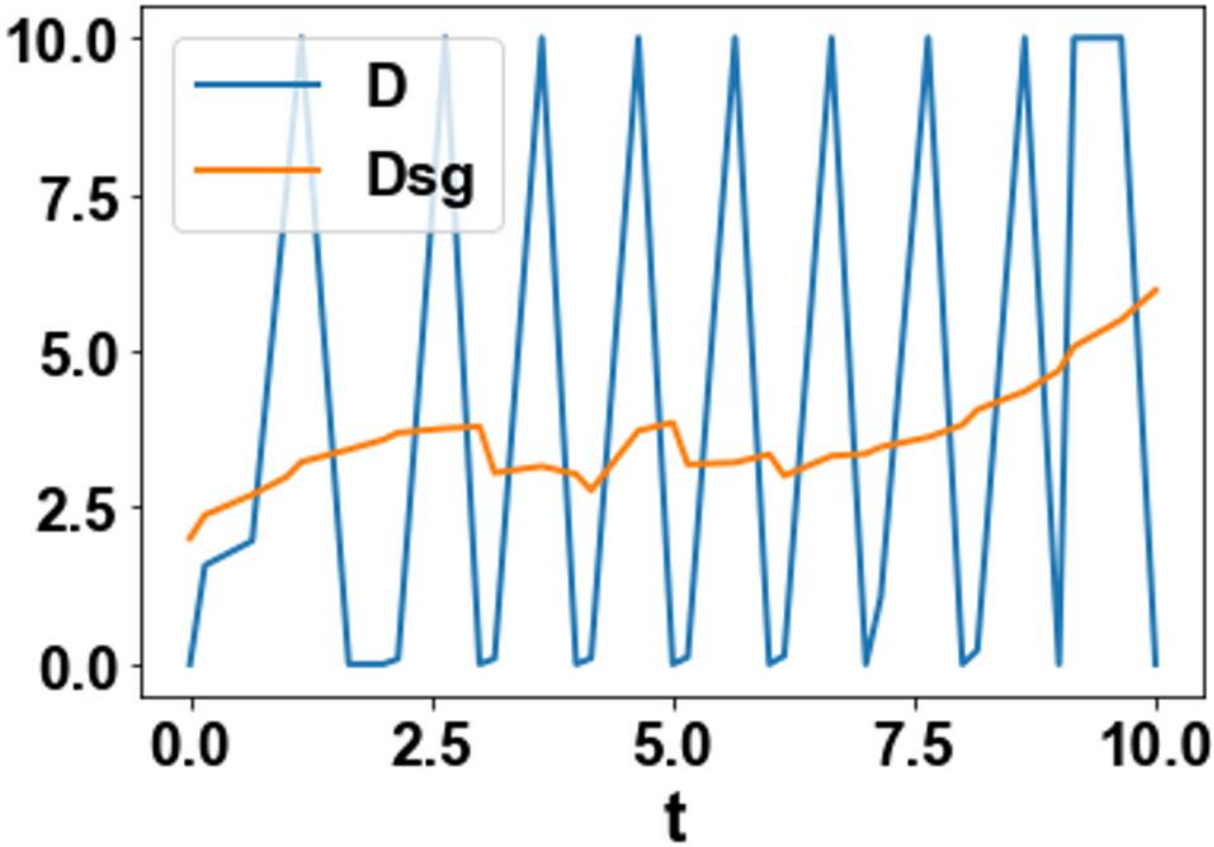

Figure 3h. Optimal Control Saccaharomyces Cerevisiae (D, DSG profiles, with Hopf penalty).

The observed increase in product formation in Zymomonas mobilis and Saccharomyces cerevisiae fermentations after the imposition of a Hopf penalty function can be explained by the interplay among nonlinear dynamics, stability, and process performance.

The optimal control problem was solved over a finite time horizon of $t_f = 10$, with initial conditions for all variables except the input streams $C_{S0}; G_0$ being 0. The control variable, corresponding to the dilution rate, was initialized at zero and bounded within the interval $[0, 5]$. The system of differential-algebraic equations was discretized using orthogonal collocation on finite elements, with 30–100 finite elements and three collocation points per element based on a Lagrange–Radau scheme. The resulting nonlinear programming problem was solved using the IPOPT solver with default settings, with convergence tolerances adjusted to ensure numerical stability.

For the neural network surrogate, a feedforward architecture with two hidden layers of 32 neurons each and hyperbolic tangent activation functions was employed. The network was trained using a dataset generated from numerical continuation, where each data point consists of the system states, bifurcation parameter, and the maximum real part of the Jacobian eigenvalues. Input features were standardized using the training mean and standard deviation prior to training. The model was trained using a mean squared error loss function until convergence, with a maximum of 5000 iterations.

In the optimal control formulation, stability was incorporated using a soft Hopf penalty with weighting parameter $\alpha = 50$ and smoothing parameter $\epsilon = 0.01$. These values were selected to balance product maximization and stability enforcement while maintaining numerical tractability.

A Hopf bifurcation in a fermentation system indicates the change from a stable steady state to oscillations in the state variables, such as biomass, substrate, and product concentrations. If the system operates near the boundary of a Hopf bifurcation, the eigenvalues of the linearized model approach the imaginary axis, implying that disturbances decay very slowly. Although this region indicates a high rate of activity, oscillations in the system variables result.

Without the imposition of a Hopf penalty, the optimizer would drive the system to conditions that maximize production rate. In nonlinear systems, such as biochemical processes, the conditions that maximize production rate occur near the boundary of instability. Although the production rate appears high, oscillations in the system variables lead to a lower time-averaged productivity. The periodic depletion of the substrate or the temporary cessation of activity would result in a lower product formed over the entire period of operation.

The addition of the Hopf penalty function modifies the optimization landscape by penalizing solutions that approach the boundary of stability. Mathematically, this manifests as an increase in the penalty as the real part of the dominant eigenvalue approaches zero. This causes the optimizer to select an operating condition that is more deeply embedded in the stable region of the parameter space.

From a biochemical perspective, both Zymomonas mobilis and Saccharomyces cerevisiae have tightly coupled feedback mechanisms in substrate uptake, growth rate kinetics, and product inhibition. Nonlinear feedback mechanisms have a natural propensity to create regions of high metabolic activity with dynamic sensitivity. The optimization of the system to a stable state balances high metabolic activity with robust dynamic behavior.

The main result is that stability yields consistent product levels over time. Although the instantaneous levels may be reduced somewhat from those produced near the bifurcation point, the absence of oscillations increases overall product formation. Thus, the Hopf penalty improves not only stability but also the overall efficiency of the process, which shows that the optimal productivity of the nonlinear fermentation system is related to dynamic stability.

7. CONCLUSIONS

In the present research, an artificial intelligence-based approach has been proposed to avoid Hopf bifurcations during the optimal control of the dynamics of the fermentation process. The Hopf bifurcations were first identified through bifurcation analysis. This has provided an accurate characterization of the stability boundaries of the nonlinear process model. A neural network has been developed to characterize the stability indicators associated with Hopf bifurcations. The neural network's differentiability has enabled the incorporation of stability constraints into the optimal control formulation via a Pyomo-based model. The proposed methodology has provided an effective approach to avoiding oscillatory regimes while maximizing product concentration. The proposed approach has yielded improved results compared to traditional optimal control approaches that do not consider stability constraints. The proposed approach has ensured optimal process operation while avoiding oscillatory regimes. The proposed approach is applicable for the optimal control of other nonlinear biochemical and engineering processes.

REFERENCES

Bai, F. (2007). *Process oscillations in continuous ethanol fermentation with Saccharomyces cerevisiae*. Doctoral Dissertation, Department of Chemical Engineering, University of Waterloo. Waterloo, Ontario, Canada.

Beuse, M., Bartling, R., Kopmann, A., Diekmann, H., & Thoma, M. (1998). Effect of the dilution rate on the mode of oscillation in continuous cultures of Saccharomyces cerevisiae. *Journal of Biotechnology, 61*(1), 15-31. https://doi.org/10.1016/S0168-1656(98)00016-9

Bruce, L., Axford, D., Ciszek, B., & Daugulis, A. (1991). Extractive fermentation by Zymomonas mobilis and the control of oscillatory behavior. *Biotechnology Letters, 13*(4), 291-296. https://doi.org/10.1007/BF01041487

Daugulis, A. J., McLellan, P. J., & Li, J. (1997). Experimental investigation and modeling of oscillatory behavior in the continuous culture of Zymomonas mobilis. *Biotechnology and Bioengineering, 56*(1), 99-105.

Dhooge, A., Govaerts, W., & Kuznetsov, Y. A. (2003). MATCONT: A MATLAB package for numerical bifurcation analysis of ODEs. *ACM Transactions on Mathematical Software (TOMS), 29*(2), 141-164. https://doi.org/10.1145/779359.779362

Dhooge, A., Govaerts, W., Kuznetsov, Y. A., Mestrom, W., & Riet, A. M. (2003). *Cl_matcont: A continuation toolbox in Matlab*. Paper presented at the Proceedings of the 2003 ACM Symposium on Applied Computing.

Gadkar, K. G., III, F. J. D., Crowley, T. J., & Varner, J. D. (2003). Cybernetic model predictive control of a continuous bioreactor with cell recycle. *Biotechnology Progress, 19*(5), 1487-1497. https://doi.org/10.1021/bp025776d

Garhyan, P., & Elnashaie, S. (2004). Static/dynamic bifurcation and chaotic behavior of an ethanol fermentor. *Industrial & Engineering Chemistry Research, 43*(5), 1260-1273. https://doi.org/10.1021/ie030104t

Ghommidh, C., Vaija, J., Bolarinwa, S., & Navarro, J. (1989). Oscillatory behaviour of Zymomonas in continuous cultures: A simple stochastic model. *Biotechnology Letters, 11*(9), 659-664. https://doi.org/10.1007/BF01025278

Govaerts, W. J. F. (2000). *Numerical methods for bifurcations of dynamical equilibria*. Philadelphia, PA: Society for Industrial and Applied Mathematics (SIAM).

Hart, W. E., Laird, C. D., Watson, J.-P., Woodruff, D. L., Hackebeil, G. A., Nicholson, B. L., & Siirola, J. D. (2017). *Pyomo: Optimization modeling in Python* (2nd ed.). Cham, Switzerland: Springer International Publishing.

Henson, M. A. (2003). Dynamic modeling and control of yeast cell populations in continuous biochemical reactors. *Computers & Chemical Engineering, 27*(8-9), 1185-1199. https://doi.org/10.1016/S0098-1354(03)00046-2

Henson, M. A. (2005). Cell ensemble modeling of metabolic oscillations in continuous yeast cultures. *Computers & Chemical Engineering, 29*(3), 645-661. https://doi.org/10.1016/j.compchemeng.2004.08.018

Jöbses, I., Egberts, G., Luyben, K., & Roels, J. (1986). Fermentation kinetics of Zymomonas mobilis at high ethanol concentrations: Oscillations in continuous cultures. *Biotechnology and Bioengineering*, *28*(6), 868-877. https://doi.org/10.1002/bit.260280614

Jones, K. D., & Kompala, D. S. (1999). Cybernetic model of the growth dynamics of Saccharomyces cerevisiae in batch and continuous cultures. *Journal of Biotechnology*, *71*(1-3), 105-131. https://doi.org/10.1016/S0168-1656(99)00017-6

Kurtz, M. J., Henson, M. A., & Hjortsø, M. A. (2000). Nonlinear control of competitive mixed-culture bioreactors via specific cell adhesion. *The Canadian Journal of Chemical Engineering*, *78*(1), 237-247. https://doi.org/10.1002/cjce.5450780131

Kuznetsov, Y. A. (1998). *Elements of applied bifurcation theory*. NY: Springer.

Kuznetsov, Y. A. (2009). *Five lectures on numerical bifurcation analysis*. Utrecht, Netherlands: Utrecht University.

Mahecha-Botero, A., Garhyan, P., & Elnashaie, S. (2006). Non-linear characteristics of a membrane fermentor for ethanol production and their implications. *Nonlinear Analysis: Real World Applications*, *7*(3), 432-457. https://doi.org/10.1016/j.nonrwa.2005.03.010

Martegani, E., Porro, D., Ranzi, B. M., & Alberghina, L. (1990). Involvement of a cell size control mechanism in the induction and maintenance of oscillations in continuous cultures of budding yeast. *Biotechnology and Bioengineering*, *36*(5), 453-459. https://doi.org/10.1002/bit.260360504

Mhaskar, P., Hjortsø, M. A., & Henson, M. A. (2002). Cell population modeling and parameter estimation for continuous cultures of Saccharomyces cerevisiae. *Biotechnology Progress*, *18*(5), 1010-1026. https://doi.org/10.1021/bp020083i

Mulchandani, A., & Volesky, B. (1986). Modelling of the acetone-butanol fermentation with cell retention. *The Canadian Journal of Chemical Engineering*, *64*(4), 625-631. https://doi.org/10.1002/cjce.5450640413

Parker, R. S., & Doyle, F. J. (2001). Optimal control of a continuous bioreactor using an empirical nonlinear model. *Industrial & Engineering Chemistry Research*, *40*(8), 1939-1951. https://doi.org/10.1021/ie000083s

Parulekar, S. J., Semones, G. B., Rolf, M. J., Lievense, J. C., & Lim, H. C. (1986). Induction and elimination of oscillations in continuous cultures of Saccharomyces cerevisiae. *Biotechnology and Bioengineering*, *28*(5), 700-710. https://doi.org/10.1002/bit.260280509

Perego Jr, L., Dias, J. C. d. S., Koshimizu, L., de Melo Cruz, M., Borzani, W., & Vairo, M. (1985). Influence of temperature, dilution rate and sugar concentration on the establishment of steady-state in continuous ethanol fermentation of molasses. *Biomass*, *6*(3), 247-256. https://doi.org/10.1016/0144-4565(85)90044-7

Simpson, D., Kompala, D., & Meiss, J. (2009). Discontinuity induced bifurcations in a model of Saccharomyces cerevisiae. *Mathematical Biosciences*, *218*(1), 40-49. https://doi.org/10.1016/j.mbs.2008.12.005

Sridhar, L. N. (2011). Elimination of oscillations in fermentation processes. *AIChE Journal*, *57*(9), 2397-2405. https://doi.org/10.1002/aic.12457

Strässle, C., Sonnleitner, B., & Fiechter, A. (1989). A predictive model for the spontaneous synchronization of Saccharomyces cerevisiae grown in continuous culture. II. Experimental verification. *Journal of Biotechnology*, *9*(3), 191-208. https://doi.org/10.1016/0168-1656(89)90108-9

Von Meyenburg, H. K. (1973). *Stable synchrony oscillations in continuous culture of Saccharomyces cerevisiae under glucose limitation. In B. Chance, E. K. Pye, A. K. Ghosh, & B. Hess (Eds.), Biological and biochemical oscillators*. New York: Academic Press.

Wächter, A., & Biegler, L. T. (2006). On the implementation of an interior-point filter line-search algorithm for large-scale nonlinear programming. *Mathematical Programming*, *106*(1), 25-57. https://doi.org/10.1007/s10107-004-0559-y

Zhang, Y., Henson, M. A., & Kevrekidis, Y. G. (2003). Nonlinear model reduction for dynamic analysis of cell population models. *Chemical Engineering Science*, *58*(2), 429-445. https://doi.org/10.1016/S0009-2509(02)00439-6

Zhang, Y., Zamamiri, A. M., Henson, M. A., & Hjortsø, M. A. (2002). Cell population models for bifurcation analysis and nonlinear control of continuous yeast bioreactors. *Journal of Process Control, 12*(6), 721-734. https://doi.org/10.1016/S0959-1524(01)00010-5

Zhu, G.-Y., Zamamiri, A., Henson, M. A., & Hjortsø, M. A. (2000). Model predictive control of continuous yeast bioreactors using cell population balance models. *Chemical Engineering Science, 55*(24), 6155-6167. https://doi.org/10.1016/S0009-2509(00)00208-6

Online Science Publishing *is not responsible or answerable for any loss, damage or liability, etc. caused in relation to/arising out of the use of the content. Any queries should be directed to the corresponding author of the article.*